

## Discriminating a gravitational wave background from instrumental noise in the LISA detector

Massimo Tinto,\* J. W. Armstrong,† and F. B. Estabrook‡

*Jet Propulsion Laboratory, California Institute of Technology, Pasadena, California 91109*

(Received 11 September 2000; published 4 December 2000)

The multiple Doppler readouts available with the Laser Interferometer Space Antenna (LISA) permit simultaneous formation of several observables. All are independent of laser phase fluctuations, but have different couplings to gravitational waves and the various LISA instrumental noises. Comparison, for example, of the Michelson interferometer observable with the fully symmetric Sagnac data-type allows discrimination between a confusion-limited gravitational wave background and instrumental noise.

DOI: 10.1103/PhysRevD.63.021101

PACS number(s): 04.80.Nn, 07.60.Ly, 95.55.Ym

The Laser Interferometer Space Antenna (LISA) is a proposed mission which will use coherent laser beams exchanged between three remote widely separated spacecraft to detect and study low-frequency ( $10^{-4}$ –1 Hz) cosmic gravitational radiation. Modeling each spacecraft as carrying lasers, beam splitters, photodetectors and drag-free proof masses on each of two optical benches, it has been shown that the six measured time series of Doppler shifts of the one-way laser beams between spacecraft pairs, and the six measured shifts between adjacent optical benches on each spacecraft, can be combined, with suitable time delays, to cancel the otherwise overwhelming phase noise of the lasers ( $\Delta\nu/\nu \approx 10^{-13}$ ) to a level  $h \approx \Delta\nu/c \approx 10^{-23}$ . This level is set by both the buffeting of the drag-free proof masses inside each optical bench, and the shot noise at the photodetectors.

Very strong galactic binary signals are expected to be individually detectable by LISA. Particularly at low Fourier frequencies (say 0.1–8 MHz), however, it is expected that there will be many sources radiating within each Fourier resolution bin [1–3]. These latter signals will not be detectable individually, and will form a continuum which could mimic — and thus be confused with — instrumental noise. The level of this continuum could be in the range  $10^{-20}$ – $10^{-23}$  [1–3]. A measurement of the amplitude and frequency dependence of this background, and its variation with its position in the sky, will confirm or disprove estimates of galactic binary system populations, including their distributions in the galaxy [4]. Since these galactic binary populations are virtually guaranteed, the detection of their signals could be the first direct detection of gravitational waves.

For this measurement it is very desirable that competing proof-mass or other instrumental noises not only be characterized and calibrated before flight, but also be measured in the actual flight configuration while data are being taken. In contrast with Earth-based, equi-arm interferometers for gravitational wave detection, LISA will have multiple readouts, and these data can be combined differently to give measurements not only insensitive to laser phase fluctuations and

optical bench motions, but also with different sensitivities to gravitational waves and the remaining system noise [5–7].

This Rapid Communication briefly discusses two laser-and-optical-bench-noise-free combinations of the LISA readouts, previously denoted  $\zeta$  (or Sagnac) and  $X$  (or Michelson), that have very different responses to the gravitational wave background, but comparable responses to instrumental noise sources [5–7].

In Fig. 1 the six Doppler beams between the LISA spacecraft are symbolically shown, together with the six Doppler readouts  $y_{ij}$  ( $i, j = 1, 2, 3$ ), recorded when each transmitted beam is mixed with the laser light of the receiving optical bench. Delay times for travel between the spacecraft must be carefully accounted for when combining these data. Six further data streams, denoted  $z_{ij}$  ( $i, j = 1, 2, 3$ ), are generated internally to monitor both lack of rigidity and laser synchronization between the independent optical benches at each spacecraft. We use all the conventions and definitions of Ref. [7], where a number of laser-and-bench-noise-free combinations of the data ( $y_{ij}$ ,  $z_{ij}$ ) were identified.

The simplest such combination,  $\zeta$ , uses all the data of Fig. 1 symmetrically:

$$\begin{aligned} \zeta = & y_{32,2} - y_{23,3} + y_{13,3} - y_{31,1} + y_{21,1} - y_{12,2} \\ & + \frac{1}{2} (-z_{13,21} + z_{23,12} - z_{21,23} + z_{31,23} - z_{32,13} + z_{12,13}) \\ & + \frac{1}{2} (-z_{32,2} + z_{12,2} - z_{13,3} + z_{23,3} - z_{21,1} + z_{31,1}). \end{aligned} \quad (1)$$

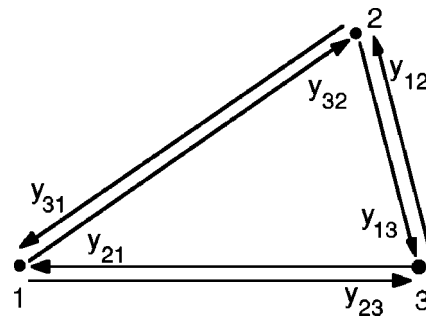


FIG. 1. Schematic illustration of the six laser links in LISA. The  $y_{ij}$  are the fractional frequency fluctuations in the Doppler links. All six of these links can be combined to produce the Sagnac data combination,  $\zeta$ , which is relatively insensitive to gravitational radiation.

\*Electronic address: massimo.tinto@jpl.nasa.gov

†Electronic address: john.w.armstrong@jpl.nasa.gov

‡Electronic address: frank.b.estabrook@jpl.nasa.gov

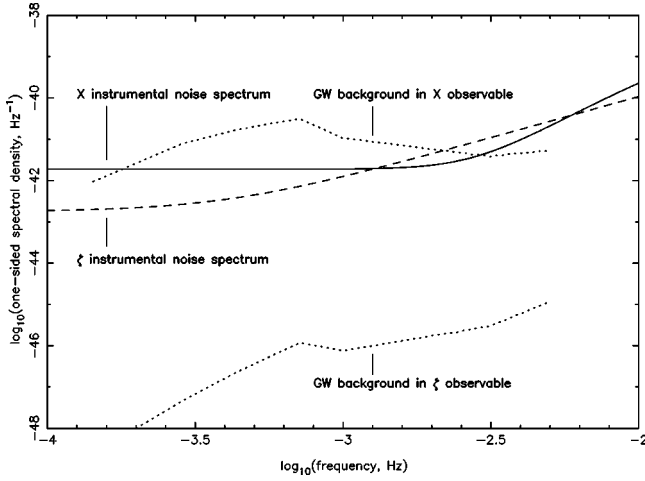


FIG. 2. Fractional Doppler frequency instrumental noise power spectra for data combinations  $X$  (solid line) and  $\zeta$  (dashed line). These are derived from the transfer functions for  $X$  and  $\zeta$  to instrumental noises and the nominal LISA spectra for individual proof mass noise [ $3 \times 10^{-15}$  (m/sec<sup>2</sup>)/ $\sqrt{Hz}$ ] and one-way optical path noise [ $20 \times 10^{-12}$  m/ $\sqrt{Hz}$ ], converted to fractional Doppler spectra. Also plotted are the spectral responses of  $X$  and  $\zeta$  to the expected stochastic gravitational wave background as discussed by Bender and Hils [1], and Hils [2]. Using  $\zeta$  to measure on-orbit instrumental noise allows a gravitational wave background in  $X$  to be either uniquely determined or bounded.

The comma notation indicates time-delays along the arms of the 3-spacecraft configuration

$$y_{32,2} \equiv y_{32}(t - L_2), \quad (2)$$

and so forth (units in which  $c = 1$ ).

The transfer functions of  $\zeta$  to instrumental noises and to gravitational waves were calculated in [6] and [7]. Using current specifications for random velocities expected for the six drag-free proof masses, for fluctuations due to shot-noise at the readouts and for beam-pointing noise, the expected noise power spectra can then be computed. The resulting instrumental noise power spectrum for  $\zeta$  is shown in Fig. 2. Also shown there is the computed power spectrum of  $\zeta$ , averaged over the sky and elliptical polarization states, that would result from a stochastic background originated by an ensemble of galactic binary systems, based on Fig. 2 of Bender and Hils [1].

In Fig. 3 the laser- and optical-bench-noise-free data combination,  $X$ , is illustrated; only four data streams are required. If low-noise optical transponders can be used at spacecraft 2 and 3, then only the two readouts on board spacecraft 1 are needed [5,8]. This combination is equivalent to an (unequal arm) Michelson interferometer. In general it is given by

$$\begin{aligned} X = & y_{32,322} - y_{23,233} + y_{31,22} - y_{21,33} + y_{23,2} - y_{32,3} + y_{21} - y_{31} \\ & + \frac{1}{2} (-z_{21,2233} + z_{21,33} + z_{21,22} - z_{21}) \\ & + \frac{1}{2} (+z_{31,2233} - z_{31,33} - z_{31,22} + z_{31}). \end{aligned} \quad (3)$$

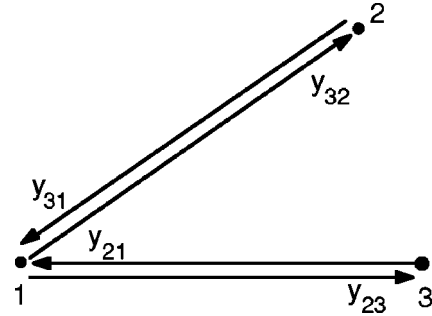


FIG. 3. As in Fig. 1, but for the links involved in the unequal-arm Michelson interferometer combination,  $X$ , which is much more sensitive to gravitational radiation than  $\zeta$ .

The expected instrumental noise power spectrum in  $X$ , using Eq. (3) and the appropriate transfer functions [6,7], is shown in Fig. 2. Also shown is the anticipated galactic binary confusion spectrum [1], which would be observed in  $X$ . It is clear that a comparison of  $X$  and  $\zeta$  may allow the background to be discriminated against instrumental noise.

LISA will have an equilateral configuration with  $L_1 = L_2 = L_3 = L \approx 17$  sec. In the frequency band of interest (0.1–8 MHz), the expressions for the Fourier transforms of the gravitational wave signals  $\tilde{X}^{gw}(f)$ ,  $\tilde{\zeta}^{gw}(f)$  and the power spectral densities of the system noises in  $X$  and  $\zeta$ ,  $S_{Xnoise}(f)$ ,  $S_{\zeta noise}(f)$ , can be Taylor-expanded in the dimensionless quantity  $fL$ . The first non-zero terms are

$$\tilde{X}^{gw}(f) \approx 2(2\pi i f L)^2 [\hat{n}_3 \cdot \tilde{\mathbf{h}}(f) \cdot \hat{n}_3 - \hat{n}_2 \cdot \tilde{\mathbf{h}}(f) \cdot \hat{n}_2], \quad (4)$$

$$\begin{aligned} \tilde{\zeta}^{gw}(f) \approx & \frac{1}{12} (2\pi i f L)^3 [(\hat{k} \cdot \hat{n}_1)(\hat{n}_1 \cdot \tilde{\mathbf{h}}(f) \cdot \hat{n}_1) \\ & + (\hat{k} \cdot \hat{n}_2)(\hat{n}_2 \cdot \tilde{\mathbf{h}}(f) \cdot \hat{n}_2) \\ & + (\hat{k} \cdot \hat{n}_3)(\hat{n}_3 \cdot \tilde{\mathbf{h}}(f) \cdot \hat{n}_3)], \end{aligned} \quad (5)$$

$$\begin{aligned} S_{Xnoise}(f) \equiv & S_{Xproofmass}(f) + S_{Xopticalpath}(f) \\ \approx & 16[S_1(f) + S_{1*}(f) + S_3(f) + S_{2*}(f)](2\pi f L)^2 \\ & + 4[S_{32}(f) + S_{23}(f) + S_{31}(f) + S_{21}(f)] \\ & \times (2\pi f L)^2 \end{aligned} \quad (6)$$

$$\begin{aligned} S_{\zeta noise}(f) \approx & [S_1(f) + S_2(f) + S_3(f) + S_{1*}(f) + S_{2*}(f) \\ & + S_{3*}(f)](2\pi f L)^2 + [S_{32}(f) + S_{23}(f) \\ & + S_{31}(f) + S_{21}(f) + S_{13}(f) + S_{12}(f)], \end{aligned} \quad (7)$$

where we have denoted by  $S_{Xproofmass}(f)$  and  $S_{Xopticalpath}(f)$  the aggregate contributions to the power spectrum of the noise in the response  $X$  from the proof mass and optical path noises, respectively. The expressions in square brackets in Eqs. (4) and (5) incorporate LISA antenna responses [6], and are of the same order of magnitude. The proof mass Doppler noise spectra  $S_i(f)$ ,  $S_{i*}(f)$  ( $i = 1, 2, 3$ ) will be designed to a nominal power spectral level  $S^0(f) = 2.5 \times 10^{-48} [f/1Hz]^{-2} \text{ Hz}^{-1}$  [7,8], while the optical path noise

spectra  $S_{ij}(f)$ , ( $i, j = 1, 2, 3, i \neq j$ ), which includes shot noises at the photo detectors and beam pointing noise [7], are expected to be equal to a nominal spectrum  $S^1(f) = 1.8 \times 10^{-37} [f/1\text{Hz}]^2$ . Both these noise sources will be estimated before launch, but could be larger when the in-orbit data will be taken.

First consider the responses to the gravitational wave signal, given in Eqs. (4) and (5). At  $f = 10^{-3}$  Hz, for instance (so  $2\pi fL \approx 10^{-1}$ ), the absolute value of the coefficient in front of the squared-bracket in the  $\zeta$  response [Eq. (5)] is about three orders of magnitudes smaller than the corresponding coefficient given in the expression for  $X$  [Eq. (4)]. The power spectral densities of the noises due to the proof masses and the optical-path noise [Eqs. (6) and (7)] will only differ at most by an order of magnitude. We conclude that in this lower frequency range the LISA Sagnac response,  $\zeta$ , can be used as a gravitational wave shield. In the following we ignore the gravitational wave background contribution to  $\zeta$ .

To take quantitative advantage of this property of  $\zeta$ , consider the observed power spectral densities of  $X$  and  $\zeta$ ,

$$S_X^{obs}(f) = S_{Xgw}(f) + S_{Xproofmass}(f) + S_{Xopticalpath}(f) \quad (8)$$

$$S_\zeta^{obs}(f) = \frac{1}{16} \left[ S_{Xproofmass}(f) + \frac{S_{Xopticalpath}(f)}{(\pi fL)^2} \right] + [S_2(f) + S_{3*}(f)](2\pi fL)^2 + [S_{13}(f) + S_{12}(f)], \quad (9)$$

where in Eq. (9) we have partitioned the power spectra of the noise in the  $\zeta$  observable in terms of the power spectra of the noises in the  $X$  observable and some remaining terms that are not present in  $X$ , to emphasize commonality of some noise sources. The noise contributed by any one of the proof masses and optical-path noise sources is unlikely to be smaller than the design values,  $S^0(f)$ ,  $S^1(f)$ . From Eq. (9) we conclude that, if the magnitude of the measured power spectral density of the response  $\zeta$  is at its anticipated level  $S_\zeta^{obs}(f) = 6S^0(f)(2\pi fL)^2 + 6S^1(f)$ , then the level of the power spectral density of the noise entering into  $X$  is known. This would imply that the spectrum

$$S_{Xgw}(f) = S_X^{obs}(f) - 64S^0(f)(2\pi fL)^2 - 16S^1(f)(2\pi fL)^2 \quad (10)$$

should then be attributed to a galactic binary background of gravitational radiation. In any event, the right-hand side of Eq. (10) is an upper bound to  $S_{Xgw}$ .

If the measured spectrum of  $\zeta$  is above its anticipated design level, consider the observed spectral data of  $X$  and  $\zeta$ , differenced

$$\begin{aligned} S_X^{obs}(f) - 16S_\zeta^{obs}(f) &= S_{Xgw} - 16[S_2(f) + S_{3*}(f)](2\pi fL)^2 \\ &\quad - 16[S_{13}(f) + S_{12}(f)] - 16[S_{32}(f) \\ &\quad + S_{23}(f) + S_{31}(f) + S_{21}(f)] \\ &\quad \times [1 - (\pi fL)^2]. \end{aligned} \quad (11)$$

The coefficient of  $S_\zeta^{obs}$  has been chosen so that the noise terms on the right-hand side are all now negative-definite and can be bounded from above by their design, or nominal, values  $S^0(f)$  and  $S^1(f)$ , respectively. The result is a lower bound for experimental discrimination of the gravitational wave background spectrum

$$\begin{aligned} S_{Xgw}(f) &\geq S_X^{obs}(f) - 16S_\zeta^{obs}(f) + 32(2\pi fL)^2 S^0(f) \\ &\quad + 16[6 - (2\pi fL)^2] S^1(f). \end{aligned} \quad (12)$$

Equations similar to (11) and (12) can be written for the other two interferometer combinations,  $Y$  and  $Z$  [7]. In those equations, there will be different mixes of canceled and bounded noise sources, resulting in different gravitational wave spectrum lower bounds.

We note moreover that such bounds result not only from using  $\zeta$  with data combinations  $X$ ,  $Y$ , and  $Z$ , but also with other data types [7] such as  $\alpha$ ,  $P$ , etc. If certain of the proof masses are significantly noisier than others, this can make some of these bounding criteria preferable. As an example, the spectral difference  $S_\alpha^{obs}(f) - 9S_\zeta^{obs}(f)$  has negative-definite noise and leads to the lower bound

$$S_{\alpha gw}(f) \geq S_\alpha^{obs}(f) - 9S_\zeta^{obs}(f) + 32(2\pi fL)^2 S^0(f) + 48S^1(f). \quad (13)$$

This research was performed at the Jet Propulsion Laboratory, California Institute of Technology, under contract with the National Aeronautics and Space Administration.

- 
- [1] P. L. Bender and D. Hils, *Class. Quantum Grav.* **14**, 1439 (1997).  
 [2] D. Hils, in *Proceedings of the 2nd International LISA Symposium on the Detection and Observation of Gravitational Waves in Space*, Pasadena, California, 1998, edited by W. M. Folkner, AIP Conf. Proc. No. **456** (AIP, New York, 1998).  
 [3] D. Hils, P. L. Bender and R. F. Webbink, *Astrophys. J.* **360**, 75 (1990).  
 [4] R. F. Webbink, *Astrophys. J.* **277**, 355 (1984).

- [5] M. Tinto and J. W. Armstrong, *Phys. Rev. D* **59**, 102003 (1999).  
 [6] J. W. Armstrong, F. B. Estabrook, and M. Tinto, *Astrophys. J.* **527**, 814 (1999).  
 [7] F. B. Estabrook, M. Tinto, and J. W. Armstrong, *Phys. Rev. D* **62**, 042002 (2000).  
 [8] P. Bender, K. Danzmann, and the LISA Study Team, *Laser Interferometer Space Antenna for the Detection of Gravitational Waves, Pre-Phase A Report*, **MPQ233** (Max-Planck-Institut für Quantenoptik, Garching, 1998).